

Rheological, mechanical and corrosive properties of injection molded 17-4PH stainless steel^①

LI Yimin(李益民), K. A. Khalil, HUANG Baixun(黄伯云)

(State Key Laboratory for Powder Metallurgy, Central South University, Changsha 410083, China)

Abstract: The feedstock based on the binder 65% PW-30% EVA-5% SA has the best general rheological properties for the 17-4PH stainless steel powder. The 17-4PH stainless steel compacts sintered at 1 380 °C for 90 min have the best mechanical properties and the good microstructure with homogeneously distributed pore structure and the moderate sized grains. Whereas the compacts sintered for 60 min and 120 min show an inadequate and an over-sintered microstructure respectively. The compacts sintered at 1380 °C for 90 min have the density of 7.70 g/cm³, the strength of 1 275 MPa, the elongation of 5%, and hardness of HRC36. With the increase of sintering temperature, the density, strength and hardness increase, while the elongation decreases. The 17-4PH stainless steel has good corrosion resistance, showing an activation passivation polarization curve. But the passivation potential range is narrow and the spot corrosion potential is low, indicating a low anti-spot corrosive properties.

Key words: metal injection molding (MIM); rheological properties; mechanical properties; corrosive resistance; 17-4PH stainless steel

CLC number: TF 125.3

Document code: A

1 INTRODUCTION

Stainless steels may be defined as alloy steels containing at least 10% chromium with or without other elements. Stainless steels are more resistant to rusting and staining than plain carbon and low-alloy steels. They have superior corrosion resistance, superior resistance to oxidation and sulfidation, high strength and ductility, and good surface finish. But stainless steels are hard to machine, many intricate stainless steel parts are produced by investment casting. The stainless steel parts made by investment casting have the defects such as low dimensional tolerance, rough surface finish, element segregation. Stainless steel parts can also be made by traditional press/sinter technology. But the large porosity due to the low density leads to lower mechanical properties, inferior corrosion resistance and rough surface finish. At the same time, the traditional press/sinter technology can only produce the parts with simple shape. Metal injection molding (MIM) has been paid more and more attention because the complex-shaped parts with high performances can be cheaply manufactured by this technology^[1-8]. MIM has the particular advantage of fabricating complicated-shaped parts with the homogeneous microstructure and superior mechanical properties. MIM stainless steel parts have

been used for orthodontic brackets, electric switchbox and vending machine coin locks, read/write latch arm for hard disk drive, spacer assembly, endoscopic surgical scissors, shower valve, pump body and cavity plates, helical gear, endoscopic surgical stapler, and foldable paper hole punch etc. In recent years, the worldwide MIM sales increase by 20% to 30% per year, most of which is owing to the growth of MIM stainless steel parts^[9]. Nowadays, 316L austenitic stainless steel parts occupy most of MIM stainless steel parts. Austenitic stainless steels have relatively lower strength and hardness, and are not applicable for the parts requiring both higher mechanical properties and superior corrosion resistance. Whereas 17-4PH stainless steel is a kind of precipitation-hardening stainless steel with higher strength and hardness similar to common tool steels. The injection molding process of 17-4PH stainless steel, the rheological properties, the mechanical properties, the microstructure, and the corrosion resistance are investigated in present paper.

2 EXPERIMENTAL

2.1 Materials

The metal powder used in this study was gas atomized spherical 17-4 PH stainless steel powder with

① **Foundation item:** Project(2001AA337050) supported by National Hi-tech Research Development Program of China; project(81041) supported by the HUO Yirong Education Foundation; project(200135) supported by the Chinese National Excellent Dissertation Foundation

Received date: 2004-02-11; **Accepted date:** 2004-05-20

Correspondence: LI Yimin, Professor, PhD; Tel: +86-731-8830693; E-mail: liyimin33@yahoo.com.cn

the pycnoemeter density of 7.89 g/cm³. The chemical composition and the powder morphology are shown in Table 1 and Fig. 1 respectively. The particle size distribution was as follows: $d_{10} = 5 \mu\text{m}$, $d_{50} = 12 \mu\text{m}$, $d_{80} = 22 \mu\text{m}$. The apparent and tap density of the powder was 3.92 and 4.70 g/cm³ respectively. Four kinds of binder systems based on paraffin wax were prepared and used in this study. The minor components were poly [ethylene vinyl acetate (EVA)], high-density polyethylene (HDPE), low-density polyethylene (LDPE), and polypropylene (PP). Stearic acid (SA) was included as a surface active agent. The characteristics of the binder components and the binder compositions are shown in Table 2 and Table 3 respectively.

Table 1 Chemical composition of 17-4PH stainless steel powder (mass fraction, %)

Element	Fe	Ni	Cr	C
Minimum	69.98	3.00	15.50	0
Maximum	78.35	5.00	17.50	0.07
Element	Cu	Nb+ Ta	Mn	Si
Minimum	3.00	0.15	0	0
Maximum	5.00	0.45	1.00	1.00

Table 2 Characteristics of binder components

Component	Chemical structure	$t_m/^\circ\text{C}$	$\rho/(\text{g}/\text{cm}^3)$
PW	$\text{C}_n\text{H}_{2n+2}$	58	0.9
HDPE	$[\text{--CH}_2\text{--CH}_2]_n$	139	0.95
LDPE	$[\text{--CH}_2\text{--CH}_2]_n$	-	-
PP	$[\text{--CH} \begin{array}{c} \\ \text{CH} \end{array}]_n$	142	0.9
EVA	$[\text{--CH} \begin{array}{c} \\ \text{CH}_2 \end{array}]_x \text{--} [\text{CH}_2\text{--CH}_2]_y \text{--}]_n$	80	0.96
SA	$\text{CH}_3[\text{CH}_2]_{16}\text{COOH}$	66	0.96

Table 3 Binder composition (mass fraction, %)

Feedstock	Binder	PW	HDPE	LDPE	PP	EVA	SA
A	1	65	-	-	-	30	5
B	2	65	30	-	-	-	5
C	3	65	-	15	15	-	5
D	4	65	15	-	-	15	5

2.2 Experimental procedure

The mixing of the powder and the binder was carried out on XSM 1/20-80 rubber mixer at 175 °C to get the feedstock. The feedstock was injection molded on a BOY50T2 molding machine after the extrusion granular

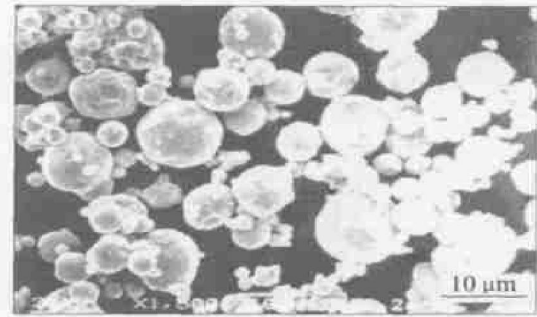


Fig. 1 SEM photograph of 17-4PH stainless steel powder

tion on a YHL04 plastic extruder. The viscosity and rheological properties of the feedstock were determined by an Instron 3211 rheometer. The standard tensile bars were prepared for the investigation of the mechanical properties and the microstructure. A rectangular specimen (43 mm × 8.4 mm × 2.7 mm) was prepared for the corrosive properties study. The solvent debinding was carried out in heptane at 40 °C. The thermal debinding and sintering were carried out in hydrogen atmosphere.

The density, hardness, tensile strength and elongation were tested, and the microstructure was observed. The corrosion resistance was determined by the mass loss immersion test and the anodic potentiometry measurement. The apparatus for the mass loss immersion test was shown in Fig. 2. The 5% hydrochloric acid solution, which is kept in 50 °C water bath, was used in this test. The samples were immersed in the hydrochloric acid solution for 88 h. The samples were taken out 5 to 6 times to measure the rate of corrosion. The corrosion rate can be calculated by the following equation,

$$R = m/(A \cdot t) \quad (1)$$

where R is the corrosion rate, m the mass loss (g), A the sample area (m²), and t the time (h). The samples for the anodic potentiometry measurement were prepared by polishing the specimen of the surface area of 10 mm × 10 mm to remove the passivating film for the exposure of 0.1 cm² area, with the other area mounted in the polystyrene. Then the samples were immersed into 0.3% NaCl solution at the temperature of (30 ± 1) °C. The solution was keeping aerated with the aeration rate of 0.5 L/min. The potentiodynamic polarization was carried out at the potential scan rate of 1 mV/s from the potential of -0.9 V.

3 RESULTS AND DISCUSSION

3.1 Rheological properties of feedstock

The relationship of shear stress and shear rate for the feedstock A, B, C and D of 64% powder loading at 135 °C is shown in Fig. 3. An MIM feedstock is generally considered to be a pseudoplastic fluid^[10,11].

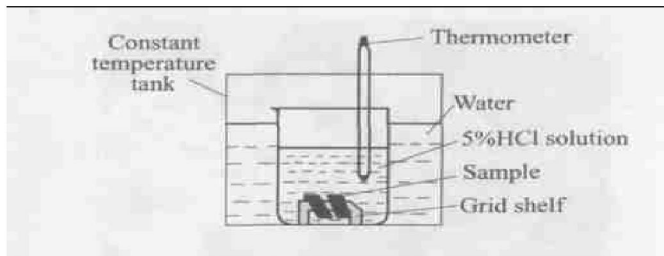


Fig. 2 Apparatus for mass loss immersion test

For a pseudoplastic fluid, there is

$$\tau = k \cdot \gamma^n \quad (2)$$

where τ is the shear stress, γ the shear rate, k a constant, n a flow behavior exponent (< 1). The value of n indicates the degree of shear sensitivity. The lower the value of n , the more quickly the viscosity of feedstock changes with shear rate. Injection molding of MIM feedstock is conducted under pressure and temperature. It is desirable that the viscosity of the feedstock should decrease quickly with increasing shear rate during injection molding. This high shear sensitivity is especially important in producing complex and delicate parts, which are leading products in the MIM industry. Plotting logarithmic shear stress against logarithmic shear rate at 135 °C as in Fig. 3, the values $n_A = 0.25$, $n_B = 0.383$, $n_C = 0.385$ and $n_D = 0.375$ can be determined. The feedstock A has the lowest value of n . Therefore, it is considered to be the best in terms of shear sensitivity. The other three kinds of feedstock have almost the same values of n .

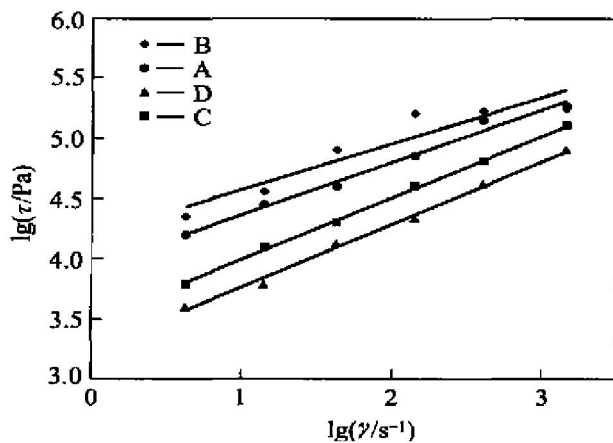


Fig. 3 Correlation of shear stress and shear rate for different kinds of feedstock

The dependence of the feedstock viscosity on temperature can be expressed by an Arrhenius equation^[12]:

$$\eta = \eta_0 \cdot \exp(E/RT) \quad (3)$$

where η_0 is the reference viscosity, E the flow activation energy, R the gas constant, and T the temperature. The value of E expresses the effect of temperature on the viscosity of the feedstock. If the value of E is low, the viscosity is not so sensitive to temperature variation. Therefore, any small fluctuation of temperature during injection molding will not result in sudden viscosity change, which could cause undue stress concentrations in molded

parts, resulting in cracking and distortion. With a shear rate of 1413 s^{-1} , which falls in the normal range of shear rates for injection molding of MIM feedstock, by plotting \ln viscosity against the reciprocal of temperature as shown in Fig. 4, the feedstock flow activation energies could be determined as: $E_A = 18.5 \text{ kJ/mol}$, $E_B = 24.9 \text{ kJ/mol}$, $E_C = 32.3 \text{ kJ/mol}$ and $E_D = 23.1 \text{ kJ/mol}$. It is found that the flow activation energy of feedstock A is the lowest, indicating that the sensitivity of its viscosity to temperature is the lowest. This feedstock could thus be injection molded on a relatively wide temperature range. The feedstocks B and D have almost the same value of flow activation energy. The feedstock C has the highest flow activation energy and is most sensitive to the temperature fluctuation.

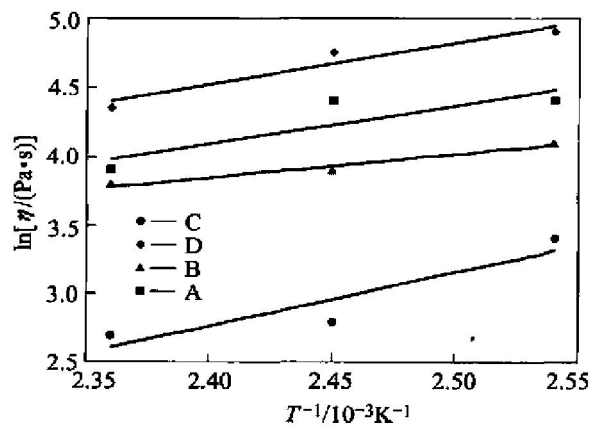


Fig. 4 Correlation of viscosity and temperature for different feedstock

The viscosity data indicate the flowability of MIM feedstock. The lower the value of the viscosity, the easier it is for a feedstock to flow. It can be seen for Figs. 3 and 4 that the feedstock C has low value of viscosity and good flowability for filling into the mold. It can be concluded from the above discussion that a feedstock with low viscosity, low flow behavior exponent, and low flow activation energy has good rheological properties and is suitable for injection molding. But there is usually a contradiction among these three requirements. A general rheological index α_{STV} ^[13], which includes the effect of the viscosity, the effect of the viscosity sensitivity to shear rate, and the effect of the viscosity sensitivity to temperature, has been proposed to evaluate the rheological properties of MIM feedstock.

$$\alpha_{STV} = \frac{1}{\eta_0} \frac{|n - 1|}{E/R} \quad (4)$$

where α_{STV} is the general rheological index. The subscripts S, T, and V of α_{STV} represent the effects of shear sensitivity, temperature sensitivity, and viscosity respectively. The higher the value of α_{STV} , the better the rheological properties are. Taking 135 °C as a reference temperature and 1413 s^{-1} as a reference shear rate, the gen-

eral rheological indexes were calculated. (α_{STV})_A = 9.1×10^{-6} , (α_{STV})_B = 4.2×10^{-6} , (α_{STV})_C = 3.1×10^{-6} and (α_{STV})_D = 5.9×10^{-6} . The feedstock A has the highest general rheological index. The feedstock A based on the binder 1# (65% PW-30% EVA-5% SA) has the best rheological properties, with the feedstock D based on the binder 4# (65% PW-15% EVA-15% HDPE-5% SA) the second, the feedstock B based on the binder 2# (65% PW-30% HDPE-5% SA) the middle, and the feedstock C based on the binder 3# (65% PW-15% LDPE-15% PP-5% SA) the last one.

3.2 Effects of sintering temperature on mechanical properties and microstructure of injection molded 17-4PH stainless steel

The mechanical properties of compacts after 90 min sintering at different temperatures of 1 345, 1 360 and 1 380 °C are shown in Table 4. It can be found that the density, the tensile strength, and the hardness increase with the sintering temperature increasing, and the elongation decrease with the temperature increasing. The 17-4PH stainless steel has a two-phase microstructure composed of about 10% ferrite and 90% martensite^[14, 15]. The change of the microstructure of the sintered compacts is shown in Fig. 5. It can be seen that the low sintering temperature results in an inadequate sintered microstructure and a higher porosity. When the sintering temperature increases from 1 345 °C to 1 380 °C, the compact density increases only by 2%, from 7.61 g/cm³ to 7.70 g/cm³, but the microstructure has a notable change. The decrease of the porosity leads to the increase of the density, hardness and strength, but the grain growth with the sintering temperature increasing results in a small decrease of the elongation.

Table 4 Mechanical properties at different sintering temperatures(90 min)

t/ °C	ρ / (g·cm ⁻³)	σ_b / MPa	δ / %	HRC
1 345	7.61	1 034	10	27
1 360	7.65	1 046	8	30
1 380	7.70	1 275	5	36

3.3 Effects of sintering time on mechanical properties and microstructure of injection molded 17-4PH stainless steel

The mechanical properties of compacts after 1380 °C sintering of 60, 90 and 120 min are shown in Table 5. When the sintering time is increased from 60 min to 90 min, the density, tensile strength, hardness are all

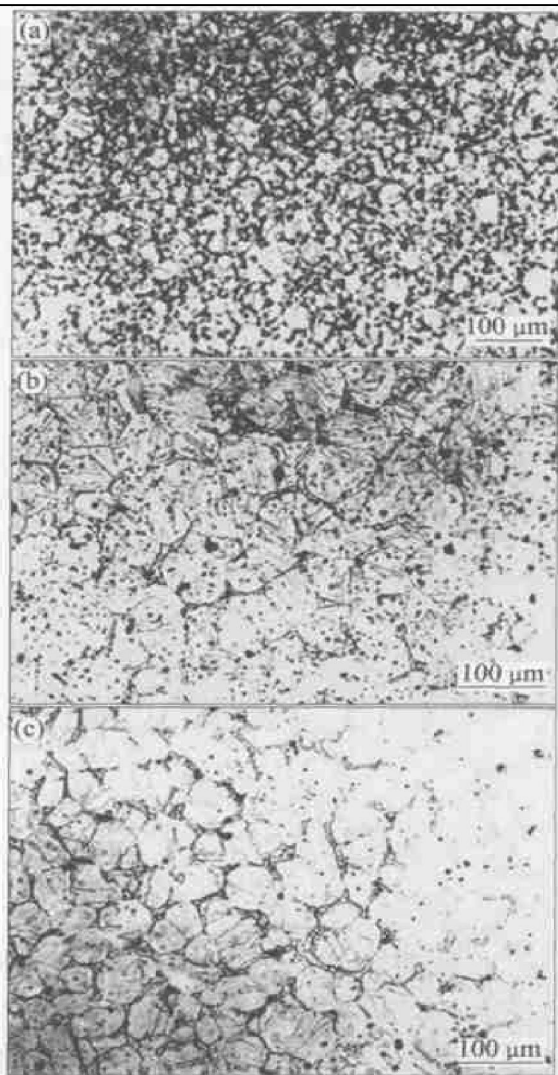
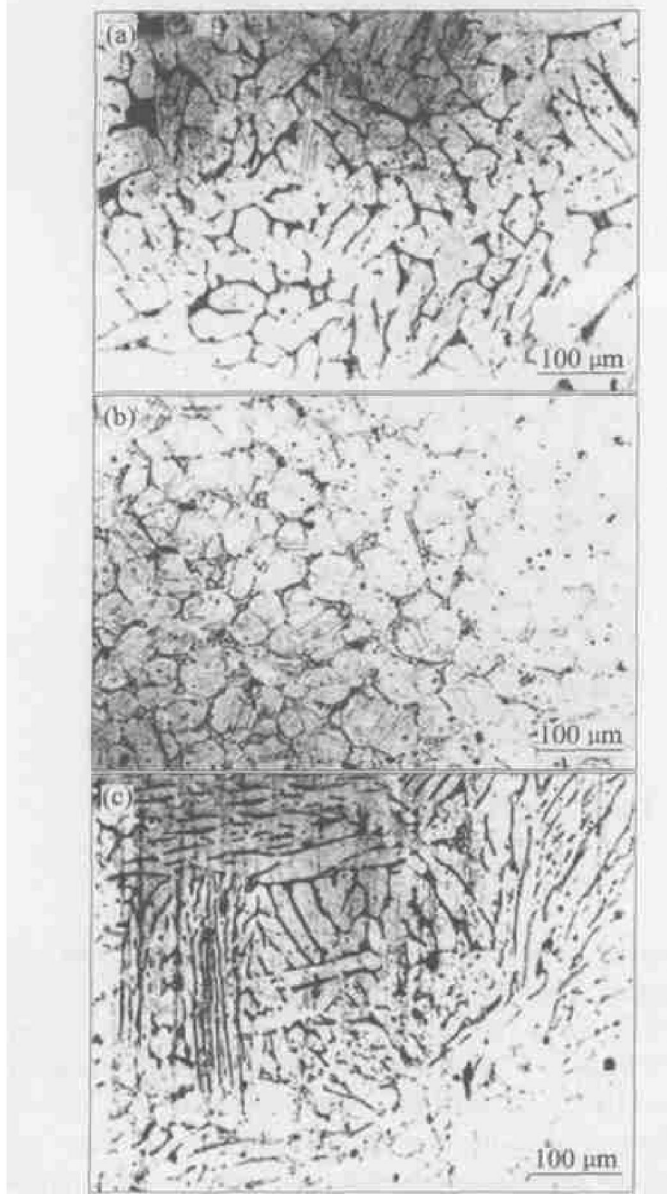


Fig. 5 Compacts microstructures at different sintering temperatures(90 min)
(a) -1 345 °C; (b) -1 360 °C; (c) -1 380 °C

increased notably, only the elongation is almost not changed. The density is increased from 7.66 g/cm³ to 7.70 g/cm³, the tensile strength is increased from 1 078 MPa to 1 275 MPa, and the hardness is increased from HRC28 to HRC36. When the sintering time is prolonged from 90 min to 120 min, the density and hardness have no more variation, whereas the tensile strength is decreased from 1 275 MPa to 1 034 MPa. The tensile strength is even lower than that of the compact with 60 min sintering. The elongation also has a little decrease after 120 min sintering. The change of the sintered microstructure with the prolongation of sintering time is shown in Fig. 6. It can be seen that the compact has a higher porosity and presents an inadequate sintered microstructure after 60 min sintering. With the prolongation of sintering time to 90 min, the compact porosity decreases. The compact has a homogeneous pore distribution and a moderate grain size. With the sintering time prolonging to 120 min, the small pores merge into large pores despite the porosity has little variation. The compact presents an over-sintered microstructure with the grain growth.

Table 5 Mechanical properties with different sintering time (1 380 °C)

Time/min	ρ /(g·cm ⁻³)	σ_y /MPa	δ /%	HRC
60	7.66	1 078	6	28
90	7.70	1 275	5	36
120	7.71	1 127	4	34

**Fig. 6** Compacts microstructures with different sintering time (1 380 °C)
(a) —60 min; (b) —90 min; (c) —120 min

3.4 Corrosion resistance

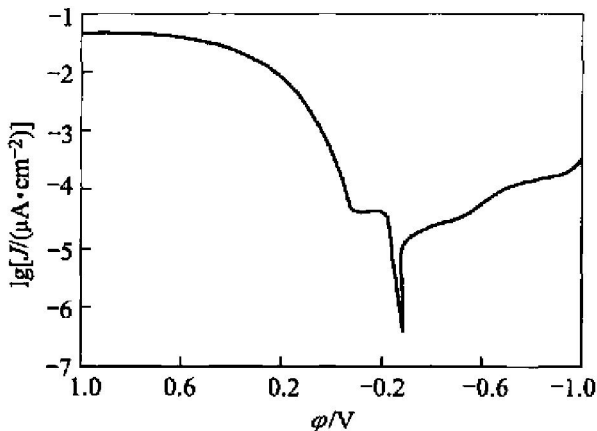
3.4.1 Mass loss immersion test in 5% HCl solution

The results of the mass loss immersion test are shown in Table 6. It can be found that MIM 17-4 PH stainless steel has good corrosion resistance. The mass losses after 24h immersion in 5% HCl solution are only 1.15 and 0.94 g/(m²·h) for the 1 360 °C and 1 380 °C sintered compacts respectively. The highest corrosion rate occurs after about 50h immersion in the acid solution.

Then the mass loss rate keeps constant till 88 h corrosion. Concerning the effects of the sintering temperature on the corrosion resistance of sintered compacts, it can be seen that the compact sintered at higher temperature has good corrosion resistance. It indicates that the compact porosity affects the corrosion resistance. The compact sintered at higher temperature has lower porosity and better corrosion resistance.

Table 6 Corrosion rates of compacts sintered at different temperatures (g·m⁻²·h⁻¹)

Corrosion time/h	1 360 °C	1 380 °C
24	1.15	0.94
40	2.72	2.22
49	2.93	2.80
71	2.71	2.70
88	2.75	2.32
Average	2.32	2.07

**Fig. 7** Potentiodynamic polarization curve in 3.5% NaCl solution

3.4.2 Anodic potentiometry measurement

The potentiodynamic polarization curve for 17-4PH stainless steel compacts in 3.5% NaCl solution is shown in Fig. 7. It can be found that MIM 17-4PH stainless steel compacts have an activation passivation polarization curve, with a relatively narrow passivation region. It is indicated that there is a passivation in NaCl solution, but the passivation potential range is narrow. The experiment results are shown in Table 7, in which φ_{corr} is the self-corrosion potential, φ_b the spot corrosion potential, φ_p the critical passivation potential, and J_p the critical passivation current density. The self-corrosion potential has a value of -0.30V. The comprehensive corrosion first occurs, followed by the passivation. The spot corrosion potential has a comparatively low value of -0.12 V, indicating a low anti-spot corrosive properties.

Table 7 Potentiodynamic polarization parameters in 3.5% NaCl solution

φ_{corr}/V	φ_b/V	φ_p/V	$J_p/(\mu A \cdot cm^{-2})$
- 0.30	- 0.12	- 0.21	- 4.2

4 CONCLUSIONS

1) The feedstock A based on the binder 1# (65% PW-30% EVA-5% SA) has the best rheological properties for 17-4PH stainless steel.

2) The density, tensile strength, and hardness of the injection molded 17-4PH stainless steel compacts increases with the sintering temperature, and the elongation decrease with the increase of temperature. The microstructure observation shows a decreased porosity and a grain growth with the increase of temperature.

3) The study of the effects of the sintering time shows that the injection molded 17-4PH compacts sintering for 90 min have the best mechanical properties, presenting a microstructure of a homogeneous pore distribution and a moderate grain size. Whereas the compacts sintered for 60 min and 120 min present an inadequate and an over-sintered microstructure respectively. The compacts sintered for 90 min on 1380 °C have the mechanical properties as $\rho = 7.70 \text{ g/cm}^3$, $\sigma_b = 1275 \text{ MPa}$, $\delta = 5\%$, and hardness of HRC36.

4) The 17-4PH stainless steel has good anticorrosive properties and long corrosion period. It has an activation-passivation polarization curve, but the passivation potential range is narrow. The spot corrosion is relatively easy to occur.

REFERENCES

[1] German R M, Hens K F. Key issues in powder injection molding[J]. Ceramic Bulletin, 1991, 70(8): 1294-1302.

- [2] German R M. Technological barriers and opportunities in powder injection molding[J]. Powder Metall Int, 1993, 25(4): 165-169.
- [3] Kulkarni K M. Future looking bright for PIM[J]. Metal Powder Report, 2000, 55(10): 40-42.
- [4] Johnson J L, German R M. PIM materials[J]. Advanced Materials and Processes, 2003, 161(4): 35-39.
- [5] Hauck Paul A. Powder injection molding: current and long term outlook[J]. International Journal of Powder Metallurgy, 2000, 36(3): 29-30.
- [6] German R M. Scientific status of metal powder injection molding[J]. International Journal of Powder Metallurgy, 2000, 36(3): 31-36.
- [7] LI Yimin, LIU Shaojun, QU Xuarrhui, et al. Thermal debinding processing of 316L stainless steel powder injection molding compacts[J]. Journal of Materials Processing Technology, 2003, 137(1-3): 65-69.
- [8] LI Yimin, JIANG Feng, ZHAO Ligang, et al. Critical thickness in binder removal process for injection molded compacts[J]. Materials Science & Engineering A, 2003, 362: 292-299.
- [9] Mark Hull. PIM97: 1st European Sym on PIM[J]. Powder Metallurgy, 1997, 40(4): 262-266.
- [10] Shah J, Nunn R E. Rheology of metal injection molding feedstock[J]. Powder Metall Int, 1987, 19(6): 38-40.
- [11] LI Yimin, QU Xuarrhui, HUANG Baixun, et al. Rheological properties of metal injection molding binder and feedstock[J]. Trans Nonferrous Met Soc China, 1999, 7(3): 103-107.
- [12] Novac O A, Anton D, Novac T. The rheological behaviour of some binder and plastisols used in injection moulding[A]. PM'94[C]. Paris, 1994, 2: 1113-1116.
- [13] LI Y, HUANG B, QU X. Viscosity and melt rheology of metal injection moulding feedstocks[J]. Powder Metall, 1999, 42(1): 6-90.
- [14] Zhang H, German R M. Powder injection molding of 17-4 PH stainless steel[A]. Booker P H, et al. Powder Injection Molding Symposium[C]. MPIF, Princeton, NJ, 1992. 219.
- [15] Murayama M, Katayama Y, Hono K. Microstructural evolution in a 17-4PH stainless steel after aging at 400 °C[J]. Metallurgical and Materials Transactions, 1999, 30(2): 345-354.

(Edited by YUAN Saqian)